1 Natural selection of glycoprotein B (gB) mutations that rescue the small

2 plaque phenotype of a fusion-impaired herpes simplex virus (HSV) mutant

- 3
- 4 Qing Fan^a, Sarah J. Kopp^a, Nina C. Byskosh^a, Sarah A. Connolly^b and Richard
- 5 Longnecker^a#
- 6
- ⁷ ^aDepartment of Microbiology-Immunology, Feinberg School of Medicine of Northwestern
- 8 University, Chicago, Illinois, USA
- 9 ^bDepartment of Health Sciences, Department of Biological Sciences, DePaul University,
- 10 Chicago, Illinois, USA
- 11
- 12 #Address correspondence to Richard Longnecker, r-longnecker@northwestern.edu
- 13
- 14 **RUNNING HEAD:** gB3A revertant mutations
- 15 ABSTRACT WORD COUNT: 250 words
- 16 TOTAL WORD COUNT: ~4900 words
- 17 **KEY WORDS**: herpes simplex virus type 1, glycoprotein B, gB, revertant, mutation,
- 18 entry, fusion
- 19

20 ABSTRACT

21 Glycoprotein B (gB) is a conserved viral fusion protein that is required for herpesvirus 22 entry. To mediate fusion with the cellular membrane, gB refolds from a prefusion to a 23 postfusion conformation. We hypothesize that an interaction between the C-terminal 24 arm and the central coiled-coil of the herpes simplex virus 1 (HSV-1) gB ectodomain is 25 critical for fusion. We previously reported that three mutations in the C-terminal arm (I671A/H681A/F683A, called gB3A) greatly reduced cell-cell fusion and that virus 26 27 carrying these mutations had a small plague phenotype and delayed entry into cells. By 28 serially passaging gB3A virus, we selected three revertant viruses with larger plagues. 29 These revertant viruses acquired mutations in gB that restore the fusion function of 30 gB3A, including gB-A683V, gB-S383F/G645R/V705I/A855V, and gB-T509M/N709H. 31 V705I and N709H are novel mutations that map to the portion of domain V that enters 32 domain I in the postfusion structure. S383F, G645R, and T509M are novel mutations 33 that map to an intersection of three domains in a prefusion model of gB. We introduced 34 these second-site mutations individually and in combination into wild-type gB and gB3A 35 to examine the impact of the mutations on fusion and expression. V705I and A855V (a 36 known hyperfusogenic mutation) restored the fusion function of gB3A, whereas S383F 37 and G645R dampened fusion and T509M and N709H worked in concert to restore gB3A fusion. The results identify two regions in the gB ectodomain that modulate the 38 39 fusion activity of gB, potentially by impacting intramolecular interactions and stability of 40 the prefusion and/or postfusion gB trimer.

41 **IMPORTANCE**

42 Glycoprotein B (gB) is an essential viral protein that is conserved in all herpesviruses 43 and is required for virus entry. gB is thought to undergo a conformational change that 44 provides the energy to fuse the viral and cellular membranes, however the details of 45 this conformational change and the structure of the prefusion and intermediate 46 conformations of gB are not known. Previously, we demonstrated that mutations in 47 the gB "arm" region inhibit fusion and impart a small plaque phenotype. Using serial 48 passage of a virus carrying these mutations, we identified revertants with restored 49 plague size. The revertant viruses acquired novel mutations in gB that restored fusion 50 function and mapped to two sites in the gB ectodomain. This work supports our 51 hypothesis that an interaction between the gB arm and the core of gB is critical for gB 52 refolding and provides details about the function of gB in herpesvirus mediated fusion 53 and subsequent virus entry.

54

55 **INTRODUCTION**

56 Herpes simplex virus (HSV) causes recurrent mucocutaneous lesions on the 57 mouth, face or genitalia and spread to the central nervous system which can lead to 58 meningitis or encephalitis (1). Infection of host cells occurs by fusion of the virion 59 envelope with a cell membrane to deliver the nucleocapsid and the viral genome into 60 the host cell. HSV entry into cells and virus-induced cell-cell fusion require the 61 coordinated action of the four viral entry glycoproteins: glycoprotein D (gD), gH, gL, and gB. The binding of gD to receptor results in a conformational change in gD that is 62 63 proposed to signal the gHgL heterodimer to trigger the fusogenic activity of gB (2-4).

64	gB is a trimeric class III viral fusion protein that is conserved across all
65	herpesviruses (5-7). Upon triggering, gB inserts into the cellular membrane and refolds
66	from a prefusion to a postfusion conformation to bring the viral and cell membranes
67	together. The structures of the postfusion forms of gB from three herpesviruses have
68	been solved (5, 8-10). To date, attempts to capture a stable prefusion form of HSV-1 gB
69	for crystallization have been unsuccessful (11). Alternative gB conformations have been
70	modeled recently using cryoelectron tomography of gB present on membranes (12, 13).
71	A prefusion model of gB has been developed using the crystal structure of the class III
72	fusion protein from vesicular stomatitis virus (VSV) (14-16).
73	Our previous site-directed mutagenesis study demonstrated that fusion was
74	impaired by mutations in an extended arm at the C-terminus of the ectodomain (domain
75	V) that packs against the coiled-coil core of gB (domain III) in the post-fusion
76	conformation (17). Alanine substitutions in three arm residues (I671A, H681A, and
77	F683A; termed gB3A in this paper) that were predicted to disrupt interactions between
78	the arm and coil greatly reduced fusion in a quantitative cell-cell fusion assay, indicating
79	that the gB arm is important for fusion. Fusion function in gB3A was restored by the
80	addition of a known hyperfusogenic mutation in the gB cytoplasmic tail, suggesting that
81	the gB3A mutations did not cause global misfolding of gB. Due to the similarity of this
82	gB coil-arm complex to the six-helix bundle of class I fusion proteins (18), we
83	hypothesized that the gB coil-arm interactions were important for the transition from a
84	prefusion to a postfusion gB conformation.
85	To further investigate the role of the gB arm region in virus entry, we generated
96	and characterized LICV/1 corruing the cD24 mutations. This cD24 views had small

86 and characterized HSV-1 carrying the gB3A mutations. This gB3A virus had small

plaques, impaired growth, and delayed penetration into cells that was restored partially
at elevated temperatures (19). These results supported our hypothesis that the gB3A
mutations alter fusion kinetics by stabilizing a prefusion or intermediate conformation of
gB or destabilizing the postfusion conformation.

91 In the present study, we passaged gB3A virus and selected for large plague variants 92 to identify mutations within gB that could restore gB3A fusion function. We selected 93 three independent revertant viruses and sequencing revealed that all three viruses 94 acquired mutations in gB. We cloned gB from the revertant viruses and introduced the 95 mutations into wild-type (WT) qB and qB3A to analyze the effect of these mutations on 96 cell surface expression and cell-cell fusion activity when coexpressed with WT qD, qH, 97 and qL. The second-site revertant mutations identified two regions that modulate the 98 fusion activity of gB3A: the C-terminus of the gB ectodomain and the intersection of 99 three domains in a model of prefusion gB.

100

101 **RESULTS**

Selection of gB3A revertant viruses. Since gB3A virus exhibited delayed entry and a small plaque phenotype (19), we used serial passage to select for second-site mutations that would rescue the gB3A plaque morphology. We hypothesized that the location of these second-site mutations would reveal gB sites of functional importance, potentially including residues that affect the stability of gB and/or interact with the domain V arm region in a prefusion or intermediate gB conformation. Since our previous study showed that truncating the cytoplasmic tail of gB3A restored its fusion activity

(17), we had reason to expect that second site mutations in gB would be able rescuethe gB3A fusion defect.

111 Three independently purified stocks of DNA from a BAC carrying gB3A (pQF297) 112 (19) were transfected individually into Vero cells expressing Cre recombinase to excise 113 the BAC backbone. Virus harvested from these cells was amplified in Vero cells to 114 generate three independent gB3A virus stocks. To select for revertant viruses 115 possessing a growth advantage linked to a restoration of fusion function, these gB3A 116 stocks were passaged serially in Vero cells. Virus harvested from each passage was 117 titered to facilitate calculation of a multiplicity of infection (MOI) of 0.01 for the next 118 passage. After serial passage, larger plagues were observed during titration and the 119 infections spread faster in culture than the parental gB3A virus. For example, prior to 120 passage 15, the gB3A virus stock designated 58621 required 7-15 days between 121 passages to reach full cytopathic effect (CPE). By passage 20, CPE developed at the 122 same rate for the 58621 infection and WT infections. By passage 24, the majority of 123 plaques from the 58621 infection were large.

Large plaque revertant viruses carry mutations in gB. A single large plaque revertant was selected from each of the three independently passaged gB3A stocks and the revertant virus was plaque purified. Viral DNA from the revertant viruses was used to clone and sequence the gB gene to allow us to examine the effect of gB mutations on fusion function in the absence of other viral genes that may have acquired mutations during the serial passaging. Sequencing results revealed that each revertant virus acquired distinct mutations within gB, including a single mutation A683V (isolated at

passage 6), a quadruple mutation S383F/G645R/V705I/A855V (isolated at passage 25),
and a double mutation T509M/N709H (isolated at passage 30).

Fusion restoration in the gB3A-A683V revertant. The gB3A-A683V revertant virus demonstrated a larger plaque size than the parental gB3A virus, with a plaque morphology that resembled WT HSV (Fig. 1). The A683V mutation directly changes one of the original residues mutated in gB3A. Residue 683 is an alanine in gB3A and a phenylalanine in WT gB.

138 To assess the impact of the A683V mutation on fusion, the gB gene from this 139 revertant virus was cloned into an expression vector (gB3A-A683V) with an N-terminal 140 FLAG tag added to facilitate comparison of expression levels. This valine substitution at 141 683 also was added to a FLAG-tagged version of WT gB (gB-F683V). A virus-free cell-142 cell fusion assay was used to examine mutant gB fusion function. In this assay, one set 143 of cells expressing T7 polymerase, gD, gH, gL, and version of gB is cocultured with a 144 second set of cells expressing with an HSV receptor and luciferase under the control of 145 the T7 promoter. Luciferase expression is used to quantify cell-cell fusion. As we 146 previously reported, gB3A mediated nearly undetectable fusion (Fig. 2) (17). gB3A-147 A683V partially restored fusion, compared to gB3A, consistent with the restoration of 148 plaque size exhibited by the revertant virus. gB-F683V showed reduced fusion 149 compared to WT gB, indicating that, although a valine is functional in this position, a 150 phenylalanine at this position promotes greater fusion. Interestingly, FLAG-tagged gB3A showed impaired cell surface expression compared to FLAG-tagged WT gB (Fig. 2). 151 152 This effect on gB3A expression was unexpected because the FLAG-tagged WT gB and 153 untagged WT gB have similar levels of surface expression (data not shown). The

addition of the A683V mutation to FLAG-tagged gB3A restored expression, which may
 partially account for restoration of fusion function.

Fusion restoration in the gB3A-S383F/G645R/V705I/A855V revertant. The gB3A-S383F/G645R/V705I/A855V revertant virus demonstrated a larger plaque size than the parental gB3A virus, with a plaque morphology that resembles a syncytial virus (Fig. 1). This morphology agrees with previous work that identified gB-A855V as a syncytial mutation (20, 21).

The gB gene from this quadruple mutant was cloned into the same expression vector as above (gB3A-S383F/G645R/V705I/A855V) to assay the effect of these mutations on cell-cell fusion and cell surface expression. The revertant gB carrying the four second-site mutations exhibited nearly WT levels of both cell surface expression and fusion (Fig. 3A). This restoration of fusion is consistent with restored plaque size of the revertant virus. As with the A683V mutant, the effect of the second-site mutations on the surface expression of FLAG-gB3A may contribute to enhanced fusion.

Sequencing the gB gene from earlier passages of this revertant virus that were
not plaque purified showed that the G645R and A855V mutations (present at passage
8) appeared before the S383F mutation (present at passage 10) and that the V705I
mutation appeared last (present in the final passage 25).

To examine how the four amino acid changes in the revertant virus may contribute to the restoration of plaque size, the mutations were introduced into gB singly or in combination. The four mutations were introduced individually into FLAG-tagged WT gB or gB3A. Then the four second-site mutations present in the revertant gB

176 construct were mutated individually back to their corresponding WT residues. Four

additional double mutations were also generated in the gB3A background.

178 Introduction of any one of the second-site mutations into WT gB did not affect the 179 cell surface expression levels (Fig. 3A). As expected, A855V enhanced cell-cell fusion 180 when added to WT gB (Fig. 3A, column 8). The A855V mutation was shown previously 181 to enhance cell-cell fusion (22, 23). Individual introduction of the other three second-site 182 mutations into WT gB enhanced fusion only modestly.

The addition of S383F or G645R to gB3A did not alter cell surface expression or fusion substantially. The addition of A855V to gB3A enhanced fusion to greater than WT levels (Fig. 3A, column 12), similar to the results observed in the WT gB background. Interestingly, V705I enhanced both gB3A cell surface expression and fusion (Fig. 3A, column 11).

188 When the second-site mutations present in gB3A-S383F/G645R/V705I/A855V 189 were restored individually to the corresponding WT gB residues, loss of the A855V 190 mutation resulted in greatly reduced fusion levels (Fig. 3A, column 16), as expected. 191 Loss of the V705I mutation modestly reduced both expression and fusion (column 15). 192 Loss of either the S383F or G645R second-site mutations (columns 13-14) did not 193 impact expression levels, but surprisingly fusion was enhanced compared to the revertant protein carrying all four mutations (column 4). This finding suggests that 194 195 S383F or G645R independently dampen fusion mediated by this revertant qB.

To further examine the role of these second-site mutations, four gB3A constructs carrying double mutations were created (Fig. 3A). The gB3A construct carrying both the V705I and A855V mutations showed the highest levels of fusion (Fig. 3A, column 20),

higher than those observed when A855V was added to gB3A alone (column 12),
suggesting that V705I promotes fusion in addition to A855V. A comparison of gB3AV705I/A855V (column 20) with the revertant carrying all four mutations (column 4)
confirms that S383F and G645R dampen fusion in this revertant. Similarly, a dampening
effect of S383F on fusion is apparent when comparing gB3A-S383F/A855V (column 19)
with gB3A-A855V (column 12) or gB3A-S383F/V705I (column 17) with gB3A-V705I
(column 11).

Fusion restoration in the gB3A-T509M/N709H revertant. The gB3A-206 207 T509M/N709H revertant virus demonstrated larger plagues than the parental gB3A 208 virus, with a plaque morphology resembling WT HSV (Fig. 1). Both of these mutations 209 are in the gB ectodomain and neither were previously reported to be hyperfusogenic. 210 Interestingly, in the postfusion structure of gB, T509 is a contact residue for F683, 211 located in the central trimeric coiled-coil. To examine the impact of these mutations on 212 gB expression and fusion, the gB gene from this virus was cloned into the same 213 expression vector as above (gB3A-T509M/N709H). The addition of these two mutations 214 to gB3A enhanced fusion (Fig. 4), consistent with the larger plague phenotype of this 215 virus. As with the previous two revertant gB constructs, the expression of the revertant 216 gB was enhanced compared to FLAG-gB3A, which may contribute to improved fusion 217 function. When the mutations were added individually to WT gB, neither mutation 218 enhanced fusion (Fig. 4), indicating that these mutations are not hyperfusogenic like 219 A855V. In fact, both of the mutations somewhat decreased fusion mediated by WT gB. 220 When the mutations were added individually to gB3A, no fusion was detected (Fig. 4), 221 indicating that neither mutation alone can rescue the fusion defect imparted by gB3A.

The mutations act in combination to restore fusion mediated by gB3A and are of particular interest because they have not been previously described and they map to two sites in the prefusion and postfusion gB structures that correspond with the gB3A-

- 225 S383F/G645R/V705I/A855V revertant.
- 226

227 **DISCUSSION**

228 The gB3A mutations (I671A/H681A/F683A) were designed based on the 229 postfusion structure of gB (5) to reduce interactions between the domain V arm and the 230 central coiled-coil (17). We previously showed that these mutations inhibited cell-cell 231 fusion and virus carrying these mutations exhibited a growth defect and formed 200-fold 232 smaller plaques than WT virus (19). To investigate how these gB3A mutations inhibit 233 fusion, we serially passaged BAC-derived gB3A virus to select for mutations that 234 overcome the fusion defect and restore a larger plaque size. Three revertant viruses were isolated and all three viruses carried mutations in gB3A. 235

236 To examine whether the newly acquired mutations in gB3A could account for the 237 restored plaque size, we cloned the gB genes from these viruses into expression 238 vectors. The second-site mutations enhanced gB3A cell-cell fusion, suggesting that 239 these mutations were responsible for the larger plaque size. Thus, natural selection 240 identified several second-site gB mutations that restore gB3A function. Although 241 additional mutations outside of qB also may have contributed to the restored plaque 242 size and/or growth of the revertant viruses, cloning the revertant gB genes allowed us to 243 analyze the effect of the gB mutations in isolation when coexpressed with WT gD, gH, 244 and gL.

The gB3A-A683V virus acquired a change in residue 683, one of the residues originally mutated to alanine in gB3A. Selection of this revertant mutation underscores the importance of residue 683 to gB fusion function and demonstrates that, although in WT residue 683 is a phenylalanine, a valine at this position is sufficient to promote fusion better than alanine, an amino acid with a smaller side-chain (Fig. 2A).

250 This A683V mutation was selected independently twice upon serial passage of 251 gB3A virus (data not shown). Interestingly, among the three original mutation sites, 252 A683 was the only one changed. In postfusion WT gB, I671, H681, and F683 pack 253 against the central coiled-coil of qB (Fig. 3B). The selection pressure for a substitution 254 at qB3A A683 rather than A681 can be explained by the structure, but the reason an 255 A683V mutation was selected over a revertant substitution in I671 is unclear. I671 and 256 F683 contact the coil more extensively than H681, with I671 and F683 contacting six 257 and five coil residues, respectively, whereas H681 contacts only three coil residues (5). The side-chain atoms of I671 and F683 make 14 and 13 contacts with the coil, 258 259 respectively, whereas the side-chain atoms of H681 make only seven contacts. The 260 specific importance of I671 and F683 was apparent when we previously showed that 261 individually mutating F683 or I671 alanine impairs fusion more than mutating H681 (17). 262 The gB3A-S383F/G645R/V705I/A855V virus retained the original three alanine 263 mutations and acquired four additional mutations, including A855V, a known 264 hyperfusogenic mutation located in the cytoplasmic tail of gB (22). By analyzing 265 individual mutations, we confirmed that A855V alone enhances both gB3A and WT gB 266 fusion (Fig. 3A). A855V and G645R mutations were the first mutations acquired in the 267 revertant virus, present by passage 8. The larger plaque phenotype was apparent at

268 this early passage, consistent with A855V being primarily responsible for the large 269 plaque phenotype. The structure of the gB cytoplasmic tail was solved recently (24) and 270 it forms a trimer that is proposed to stabilize prefusion gB, functioning as a clamp. 271 Residue 855 lies within a long helix that angles upwards toward the membrane. 272 Mutation of this residue may enhance fusion by weakening the trimerization of the 273 cytoplasmic domain. Alternatively, this residue is on the periphery of the cytoplasmic 274 domain and it could serve as a site of interaction with the gH cytoplasmic tail (24). 275 Interestingly, S383F or G645R independently appear to dampen fusion. This may 276 seem counterintuitive initially, however maximal levels of fusion do not correlate 277 necessarily with maximal titers. For example, virus complemented with hyperfusogenic 278 gB yields lower viral titers than WT gB (17, 25, 26). The S383F and G645R mutations 279 may provide a selective advantage to the revertant virus by preserving infectious virus 280 production in the presence of the hyperfusogenic A855V mutation and the boosting titer 281 of this virus. Although S383 and G645 are far apart in the postfusion structure of gB 282 (Fig. 3B), they are located close to one another in a prefusion model of gB (Fig. 3C) 283 (14), is based on the prefusion structure of the VSV fusion protein (15). S383 and G645 284 sit at the intersection of domains II, III, and IV, suggesting the possibility that mutations 285 in these residues impact interdomain interactions that stabilize prefusion gB. 286 G645 lies in the middle of a stretch of three glycines. Recently, a mutation very 287 similar to G645R was selected by serial passage of a gL-null pseudorabies virus (PRV) 288 strain (27). gL-null PRV can spread cell-to-cell and passage of this virus selected for 289 several second site mutations, including PRV gB G672R. This PRV gB mutation lies in

a residue that corresponds to the HSV-1 gB glycine immediately adjacent to G645. PRV

gB G672R was shown to be a modestly hyperfusogenic mutation when added to WTPRV gB.

In the postfusion gB structure, S383 maps in the same plane as residues H681 and F683 (Fig. 3B), presenting the possibility that replacing this small polar serine with a large hydrophobic phenylalanine may impact local interactions and alter how the arm packs against the coiled-coil in gB3A.

297 The V705I mutation enhanced surface expression levels, restoring the gB3A 298 expression defect (Fig. 3A). Greater surface expression may account for some of the 299 restoration of fusion function observed when V705I was added to gB3A. V705I also 300 appears to boost to gB3A fusion function directly, since the addition of V705I/A855V to 301 gB3A resulted in greater levels of fusion than the addition of A855V alone, despite 302 similar levels of surface expression for both constructs (Fig. 3A, columns 12 and 20). 303 V705I does not impact WT gB function, indicating that the addition of this larger hydrophobic side chain enhances gB3A fusion in a specific manner. Interestingly, the 304 305 revertant virus acquired the V705I mutation after the other three mutations. The addition 306 of V705I boosts cell-cell fusion activity compared to gB3A-S383F/G645R/A855V (Fig. 307 3A, columns 4 and 15), bringing it to the WT gB levels, potentially the optimal level for 308 virus replication. V705 lies in domain V of gB, downstream from the three alanine 309 mutations. In the postfusion structure of gB, V705 enters the core of domain I, the 310 domain that includes the fusion loops and interacts with the host cell membrane (Fig. 311 3B). Mutation of V705 may influence the conformation of domain I or the refolding of 312 gB3A into a postfusion conformation.

313 Like the quadruple mutant revertant virus, the gB3A-T509M/N709H revertant 314 virus also retained the original three alanine mutations and acquired additional 315 mutations that restored fusion function. Unlike the previous revertant, both T509M and 316 N709H were required to restore qB3A function and neither mutation was 317 hyperfusogenic in WT gB background. Remarkably, N709 is located near V705 in the 318 postfusion structure (Fig. 4B), in the portion of domain V that penetrates domain I. The 319 location of this mutation supports the importance of this region for gB fusion function. 320 Similar to V705I, N709H enhanced gB3A expression specifically, suggesting a specific 321 effect of this region on the gB3A structure. 322 T509 is a contact residue for F683 and is located in the central trimeric coiled-coil 323 of postfusion gB (Fig. 4B). Although T509M did not restore gB3A fusion on its own, the 324 substitution of a larger hydrophobic side chain at this position may partially restore an 325 interaction between the gB arm and coil. Strikingly, in the prefusion gB model, T509 lies 326 in at the intersection of domains II, III, and IV (Fig. 4C), near the location of S383 and 327 G645 (Fig. 3C). Thus, mutations in this region were selected independently in two

328 revertant viruses, suggesting that the interdomain interactions at this site may impact gB329 refolding during fusion.

We hypothesized that an interaction between the arm and coil regions of gB is important for gB refolding and we demonstrated that fusion is impeded by gB3A mutations that were designed to disrupt that interaction. Using *in vitro* evolution to select revertant viruses, we identified two gB regions that influence gB3A, including the Cterminal region of domain V in postfusion gB (residues I705 and N709) and the intersection of domains II, III, and IV in prefusion gB (residues S383, G645, and T509).

336 Mutations at these residues may compensate for the gB3A fusion defect by 337 destabilizing gB3A to reduce a kinetic barrier to fusion and/or enhancing gB expression. 338 To investigate how other viral proteins regulate and/or trigger gB fusion activity, future 339 work will select for revertant mutations outside of gB by passaging gB3A virus in cells 340 that express gB3A as a cellular protein. 341 342 MATERIALS AND METHODS 343 Cells and antibodies. Chinese hamster ovary (CHO-K1; American Type Culture 344 Collection (ATCC, USA)) cells were grown in Ham's F12 medium supplemented with 345 10% fetal bovine serum (FBS) (ThermoFisher Scientific, USA). Vero cells (ATCC, USA) 346 and Vero-cre cells that express Cre recombinase (kindly provided by Dr. Gregory Smith 347 at Northwestern University) were grown in Dulbecco modified Eagle medium (DMEM) 348 supplemented with 10% FBS, penicillin and streptomycin. The anti-FLAG MAb F1804 349 (Sigma) was used to assay cell surface expression. 350 **Plasmids and BACs.** Previously described plasmids expressing HSV-1 KOS 351 strain gB (pPEP98), gD (pPEP99), gH (pPEP100) and gL (pPEP101) (28), as well as 352 nectin-1 (pBG38) (Geraghty et al, 1998) and HVEM (pBEC10) (29), were provided by 353 Dr. Spear at Northwestern University. Plasmid pQF112 encodes an N-terminally FLAGtagged version of WT HSV-1 gB (FLAG-gB) (30). Previously described BACs used in 354 355 this study include a WT HSV-1 strain F BAC (GS3217; kindly provided by Dr. Gregory 356 Smith, Northwestern University) and a BAC derived from GS3217 that encodes gB3A 357 (pQF297) (19). Both BACs carry the red fluorescence protein (RFP) TdTomato under a

358 cytomegalovirus promoter.

- 359 For this study, all gB mutants were cloned into the pFLAG-myc-CMV-21
- 360 expression vector (E5776; Sigma), substituting the gB signal sequence and adding an
- 361 N-terminal FLAG epitope. A FLAG-tagged gB3A construct with gB3A mutations
- 362 (I671A/H681A/F683A; pQF302) was subcloned from pSG5-HSVgB-
- 363 I671A/H681A/F683A (17). Three revertant gB constructs were generated by amplifying
- the gB gene from viral DNA isolated using a DNeasy Blood and Tissue Kit (Qiagen,
- 365 USA), including I671A/H681A/F683V (pQF338),
- 366 I671A/H681A/F683A/S383F/G645R/V701I/A855V (pQF343), and
- 367 I671A/H681A/F683A/T509M/N709H (pQF339). Quikchange site-directed mutagenesis
- 368 (ThermoFisher Scientific, USA) was used to introduce specific mutations into FLAG-
- 369 tagged gB3A (pQF302), including S383F (pQF319), G645R (pQF320), V705I (pQF321),
- 370 A855V (pQF322), S383F/V705I (pQF328), G645R/V705I (pQF327), S383F/A855V
- 371 (pQF324), V705I/A855V (pQF325). The mutant constructs G645R/V701I/A855V
- 372 (pQF309), S383F/V705I/A855V (pQF310), S383F/G645R/A855V (pQF311), and
- 373 S383F/G645R/V705I (pQF312) were created by using Quikchange on pQF343.
- 374 Quikchange also was used to introduce mutations into FLAG-tagged WT gB (pQF112),
- 375 including S383F (pQF305), G645R (pQF306), V705I (pQF307), A855V (pQF309),
- T509M (pQF367), and N709H (pQF369), and F683V (pQF368). The gB open reading
- 377 frame was verified by sequencing for all clones.

Virus stocks created from BAC DNA. WT HSV-1 BAC DNA (GS3217) and three independent stocks of gB3A virus BAC DNA (pQF297) were purified. The BAC DNA was transfected using Lipofectamine 2000 (Invitrogen, Carlsbad, CA) into Vero cells expressing Cre recombinase to excise the LoxP flanked BAC backbone, as previously described (19). The transfected cells were harvested and sonicated after one week for the WT BAC and three weeks for the gB3A BAC samples, based on when the majority of cells showed RFP expression. The harvested stocks were passaged once on Vero cells in roller bottles to generate virus stocks, including a WT stock and three independent gB3A stocks designated 58621, 57621, and 58632. For 58632, the virus stock was purified using three rounds of plaque purification using limiting dilution in 96 well plates.

389 Selection of gB3A-revertant viruses. Vero cells were infected with the gB3A 390 virus stocks at an MOI of 0.01. When full disruption of the monolayer by CPE was 391 observed, cells were harvested and sonicated to create a virus stock. Virus then was 392 reseeded on Vero cells at an MOI of 0.01 for serial passage. For the gB3A stocks 393 57621 and 58621, virus was passaged in 6 well plates for 18 passages and then 394 passaged in roller bottles. For gB3A stock 58632, virus was passaged directly in roller 395 bottles. Virus stocks were titered at each passage to facilitate calculation of an MOI of 396 0.01 for the next passage. When the titering step revealed large plagues, virus from a 397 single large plague was purified through three rounds of plague purification using 398 limiting dilution in 96-well plate. Prior to the emergence of larger plaques, each gB3A 399 virus passage took 14-21 days. After larger plaques were observed, full CPE was 400 achieved at 3-4 days post-infection, similar to a WT virus infection. The gB gene from 401 larger plaque (revertant) virus stocks was sequenced. At passage 6, a 58632 revertant 402 virus carrying the gB mutation A683V was isolated. At passage 25, a 58621 revertant 403 virus carrying gB mutations S383F/G645R/V705I/A855V was isolated. At passage 30, a 404 57621 revertant virus carrying gB mutations T509M/N709H was isolated.

405 Microscopy of plaque morphology. Plaques were visualized using Giemsa
 406 (Sigma-Aldrich, USA) staining after 3 days of infection and imaged with transmitted light
 407 microscopy using EVOS Cell Imaging Systems at 4x.

408 **Cell-cell fusion assay.** The fusion assay was performed as previously described 409 (28). Briefly, CHO-K1 cells were seeded in 6-well plates overnight. One set of cells 410 (effector cells) were transfected with 400 ng each of plasmids encoding T7 RNA 411 polymerase, gD, gH, gL, and either a gB construct or empty vector, using 5 µl of Lipofectamine 2000 (Invitrogen, USA). A second set of cells (target cells) was 412 413 transfected with 400 ng of a plasmid encoding the firefly luciferase gene under control of 414 the T7 promoter and 1.5 µg of either receptor (HVEM or nectin-1) or empty vector, using 415 5 µL of Lipofectamine 2000. After 6 h of transfection, the cells were detached with 416 versene and resuspended in 1.5 mL of F12 medium supplemented with 10% FBS. 417 Effector and target cells were mixed in a 1:1 ratio and re-plated in 96-well plates for 18 418 h. Luciferase activity was quantified using a luciferase reporter assay system (Promega) 419 and a Wallac-Victor luminometer (Perkin Elmer).

420 Cell-based ELISA (CELISA). To evaluate the cell surface expression of qB 421 mutants, CHO-K1 cells seeded in 96-well plates were transfected with 60 ng of empty 422 vector or a gB construct using 0.15 µl of Lipofectamine 2000 (Invitrogen) diluted in Opti-423 MEM (Invitrogen). After 24 h, the cells were rinsed with phosphate buffered saline 424 (PBS) and CELISA staining was performed as previously described (31), using the 425 primary anti-FLAG MAb F1804. After incubation with primary antibody, the cells were 426 washed, fixed, and incubated with biotinylated goat anti-mouse IgG (Sigma), followed 427 by streptavidin-HRP (GE Healthcare) and HRP substrate (BioFX).

428

429 ACKNOWLEDGMENTS

- 430 We thank Dr. Gregory Smith for providing us with the HSV-1 BAC GS3217 and Dr.
- 431 Yasushi Kawaguchi for providing the parental BAC. We thank Nan Susmarski for timely
- 432 and excellent technical assistance and members of the Longnecker laboratory for their
- 433 help in these studies. Sequencing services were performed at the Northwestern
- 434 University Genomics Core Facility. R.L. is the Dan and Bertha Spear Research
- 435 Professor in Microbiology-Immunology. This work was supported by NIH grant
- 436 CA021776 to R.L.

437

438

439 **FIGURE LEGENDS**

440 Fig. 1. Plaque size and morphology of gB3A-revertant viruses. Vero cells were infected

441 with BAC-derived WT HSV (GS3217), gB3A virus, or gB3A-revertant viruses (A683V,

442 F383S/G645R/V705I/A855V, or T509M/N709H) at an MOI of 0.01. Three days post-

443 infection, cells were stained and imaged at 4X magnification. gB3A plaques (white

444 arrow) are compared to those of WT and revertant viruses (black arrows).

445

Fig. 2. Expression of and fusion mediated by gB mutants constructs. gB residue 683

447 was mutated to valine in FLAG-tagged constructs of WT gB and gB3A. CHO-K1 cells

- 448 (effector cells) were transfected with plasmids encoding T7 polymerase, gD, gH, and gL,
- 449 plus either a version of gB or empty vector. Another set of CHO-K1 cells (target cells)
- 450 was transfected with a plasmids encoding the luciferase gene under the control of the

451 T7 promoter and either nectin-1 or HVEM receptor. One set of effector cells was used to 452 determine cell surface expression of gB by CELISA using a MAb specific for the FLAG 453 tag (white bars). Two duplicate sets of effector cells were co-cultured with the target 454 cells expressing nectin-1 (gray bars) or HVEM (black bars) and luciferase activity was 455 assayed as measure of cell-cell fusion activity. The results are expressed as a 456 percentage of wild-type FLAG-gB expression or fusion activity, after subtracting 457 background values measured in the absence gB expression (vector). The means and 458 standard deviations of at least three independent experiments are shown.

459

460 Fig. 3. Expression of and fusion mediated by gB mutant constructs derived from gB3A-461 S383F/G645R/V705I/A855V. (A) gB mutations were added to FLAG-tagged WT gB or 462 gB3A constructs, as indicated. Cell surface expression (white bars) and fusion activity 463 (gray and black bars) of the gB constructs were assayed as in Fig. 2. Column sets are 464 numbers above the graph. (B) Location of the mutated residues on postfusion gB. The 465 crystal structure of the ectodomain of postfusion is gB (PDB ID 2GUM) is shown, with 466 five domains colored, including DI (blue), DII (green), DIII (yellow), DIV (orange), and 467 DV (red). The three residues mutated in DV of gB3A are shown (red spheres). Three of 468 the mutations selected in the gB3A revertant are shown, including S383 (dark blue 469 spheres), G645 (magenta spheres), and V705 (cyan spheres). A855 is not shown 470 because it is located in the gB cytoplasmic tail. (C) Location of mutated residues on a 471 model of prefusion gB. A model of the prefusion gB ectodomain is shown (14), with four 472 domains colored as in part B. DV and the cytoplasmic tail are not present in the model, 473 thus the residues mutated in DV of gB3A, V705, and A855 are not shown.

475	Fig. 4. Expression of and fusion mediated by gB mutant constructs derived from gB3A-				
476	T509M/N709H. (A) gB mutations were added to FLAG-tagged WT gB or gB3A				
477	constructs, as indicated. Cell surface expression (white bars) and fusion activity (gray				
478	and black bars) of the gB constructs were assayed as in Fig. 2. (B) Location of mutated				
479	residues on postfusion gB. The structure of postfusion gB (PDB ID 2GUM) is shown,				
480	with the gB3A mutated residues (red spheres) and five domains colored as in Fig. 3B.				
481	The two mutations selected in the gB3A revertant are shown, including T509 (dark blue				
482	spheres) and N709 (cyan spheres). (C) Location of mutated residues on a model of				
483	prefusion gB. A model of prefusion gB $$ is shown (14), with domains colored as in Fig.				
484	2C. T509 (blue spheres) is shown. DV is not present in the model, thus N709 is not				
485	shown.				
	REFERENCES				
486	REF	ERENCES			
486 487	REF 1.	ERENCES Roizman B. 1993. The family herpesviridae, p 1-9. <i>In</i> Roizman B, Whitley RJ,			
487		Roizman B. 1993. The family herpesviridae, p 1-9. In Roizman B, Whitley RJ,			
487 488	1.	Roizman B. 1993. The family herpesviridae, p 1-9. <i>In</i> Roizman B, Whitley RJ, Lopez C (ed), The Human Herpesviruses. Raven Press Ltd., New York.			
487 488 489	1.	Roizman B. 1993. The family herpesviridae, p 1-9. <i>In</i> Roizman B, Whitley RJ, Lopez C (ed), The Human Herpesviruses. Raven Press Ltd., New York. Connolly SA, Jackson JO, Jardetzky TS, Longnecker R. 2011. Fusing			
487 488 489 490	1.	 Roizman B. 1993. The family herpesviridae, p 1-9. <i>In</i> Roizman B, Whitley RJ, Lopez C (ed), The Human Herpesviruses. Raven Press Ltd., New York. Connolly SA, Jackson JO, Jardetzky TS, Longnecker R. 2011. Fusing structure and function: a structural view of the herpesvirus entry machinery. Nat 			
487 488 489 490 491	1. 2.	 Roizman B. 1993. The family herpesviridae, p 1-9. <i>In</i> Roizman B, Whitley RJ, Lopez C (ed), The Human Herpesviruses. Raven Press Ltd., New York. Connolly SA, Jackson JO, Jardetzky TS, Longnecker R. 2011. Fusing structure and function: a structural view of the herpesvirus entry machinery. Nat Rev Microbiol 9:369-381. 			
487 488 489 490 491 492	1. 2.	 Roizman B. 1993. The family herpesviridae, p 1-9. <i>In</i> Roizman B, Whitley RJ, Lopez C (ed), The Human Herpesviruses. Raven Press Ltd., New York. Connolly SA, Jackson JO, Jardetzky TS, Longnecker R. 2011. Fusing structure and function: a structural view of the herpesvirus entry machinery. Nat Rev Microbiol 9:369-381. Eisenberg RJ, Atanasiu D, Cairns TM, Gallagher JR, Krummenacher C, 			
487 488 489 490 491 492 493	1. 2.	 Roizman B. 1993. The family herpesviridae, p 1-9. <i>In</i> Roizman B, Whitley RJ, Lopez C (ed), The Human Herpesviruses. Raven Press Ltd., New York. Connolly SA, Jackson JO, Jardetzky TS, Longnecker R. 2011. Fusing structure and function: a structural view of the herpesvirus entry machinery. Nat Rev Microbiol 9:369-381. Eisenberg RJ, Atanasiu D, Cairns TM, Gallagher JR, Krummenacher C, Cohen GH. 2012. Herpes virus fusion and entry: a story with many characters. 			

497 5	5.	Heldwein EE, L	ou H, Bender.	FC, Cohen Gl	H, Eisenberg R	J, Harrison SC.
-------	----	----------------	---------------	--------------	----------------	-----------------

- 498 2006. Crystal structure of glycoprotein B from herpes simplex virus 1. Science
- 499 **313:**217-220.
- 500 6. Cooper RS, Heldwein EE. 2015. Herpesvirus gB: A Finely Tuned Fusion
- 501 Machine. Viruses **7:**6552-6569.
- 502 7. Backovic M, Jardetzky TS. 2009. Class III viral membrane fusion proteins. Curr
 503 Opin Struct Biol 19:189-196.
- 504 8. Backovic M, Longnecker R, Jardetzky TS. 2009. Structure of the Epstein-Barr
- 505 virus glycoprotein B. Proc Natl Acad Sci USA Accepted.
- 506 9. Burke HG, Heldwein EE. 2015. Correction: Crystal Structure of the Human
- 507 Cytomegalovirus Glycoprotein B. PLoS Pathog **11**:e1005300.
- 508 10. Chandramouli S, Ciferri C, Nikitin PA, Calo S, Gerrein R, Balabanis K,
- 509 Monroe J, Hebner C, Lilja AE, Settembre EC, Carfi A. 2015. Structure of
- 510 HCMV glycoprotein B in the postfusion conformation bound to a neutralizing
- 511 human antibody. Nat Commun **6:**8176.
- 512 11. Vitu E, Sharma S, Stampfer SD, Heldwein EE. 2013. Extensive mutagenesis of
- 513 the HSV-1 gB ectodomain reveals remarkable stability of its postfusion form. J
- 514 Mol Biol **425:**2056-2071.
- 515 12. Zeev-Ben-Mordehai T, Vasishtan D, Hernandez Duran A, Vollmer B, White P,
- 516 **Prasad Pandurangan A, Siebert CA, Topf M, Grunewald K.** 2016. Two distinct
- 517 trimeric conformations of natively membrane-anchored full-length herpes simplex
- 518 virus 1 glycoprotein B. Proc Natl Acad Sci U S A **113:**4176-4181.

519	13.	Fontana J, Atanasiu D, Saw WT, Gallagher JR, Cox RG, Whitbeck JC,
520		Brown LM, Eisenberg RJ, Cohen GH. 2017. The Fusion Loops of the Initial
521		Prefusion Conformation of Herpes Simplex Virus 1 Fusion Protein Point Toward
522		the Membrane. MBio 8.
523	14.	Gallagher JR, Atanasiu D, Saw WT, Paradisgarten MJ, Whitbeck JC,
524		Eisenberg RJ, Cohen GH. 2014. Functional Fluorescent Protein Insertions in
525		Herpes Simplex Virus gB Report on gB Conformation before and after Execution
526		of Membrane Fusion. Plos Pathogens 10 .
527	15.	Roche S, Rey FA, Gaudin Y, Bressanelli S. 2007. Structure of the Prefusion
528		Form of the Vesicular Stomatitis Virus Glycoprotein G. Science 315: 843-848.
529	16.	Backovic M, Longnecker R, Jardetzky TS. 2009. Structure of a trimeric variant
530		of the Epstein-Barr virus glycoprotein B. Proc Natl Acad Sci U S A 106:2880-
531		2885.
532	17.	Connolly SA, Longnecker R. 2012. Residues within the C-terminal arm of the
533		herpes simplex virus 1 glycoprotein B ectodomain contribute to its refolding
534		during the fusion step of virus entry. J Virol 86:6386-6393.
535	18.	White JM, Delos SE, Brecher M, Schornberg K. 2008. Structures and
536		mechanisms of viral membrane fusion proteins: multiple variations on a common
537		theme. Crit Rev Biochem Mol Biol 43: 189-219.
538	19.	Fan Q, Kopp SJ, Connolly SA, Longnecker R. 2017. Structure-Based
539		Mutations in the Herpes Simplex Virus 1 Glycoprotein B Ectodomain Arm Impart
540		a Slow-Entry Phenotype. MBio 8.

541 20. Engel JP, Boyer EP, Goodman JL. 1993. Two novel single amino acid syncytial

- 542 mutations in the carboxy terminus of glycoprotein B of herpes simplex virus type
- 543 1 confer a unique pathogenic phenotype. Virology **192:**112-120.
- 544 21. Haanes EJ, Nelson CM, Soule CL, Goodman JL. 1994. The UL45 gene
- 545 product is required for herpes simplex virus type 1 glycoprotein B-induced cell
- 546 fusion. JVirol **68:**5825-5834.
- 547 22. Silverman JL, Greene NG, King DS, Heldwein EE. 2012. Membrane
- 548 requirement for folding of the herpes simplex virus 1 gB cytodomain suggests a
- 549 unique mechanism of fusion regulation. J Virol **86:**8171-8184.
- 550 23. Baghian A, Huang L, Newman S, Jayachandra S, Kousoulas KG. 1993.
- 551 Truncation of the carboxy-terminal 28 amino acids of glycoprotein B specified by
- 552 herpes simplex virus type 1 mutant amb1511-7 causes extensive cell fusion.
- 553 JVirol **67:**2396-2401.
- 554 24. Cooper RS, Georgieva ER, Borbat PP, Freed JH, Heldwein EE. 2018.
- 555 Structural basis for membrane anchoring and fusion regulation of the herpes

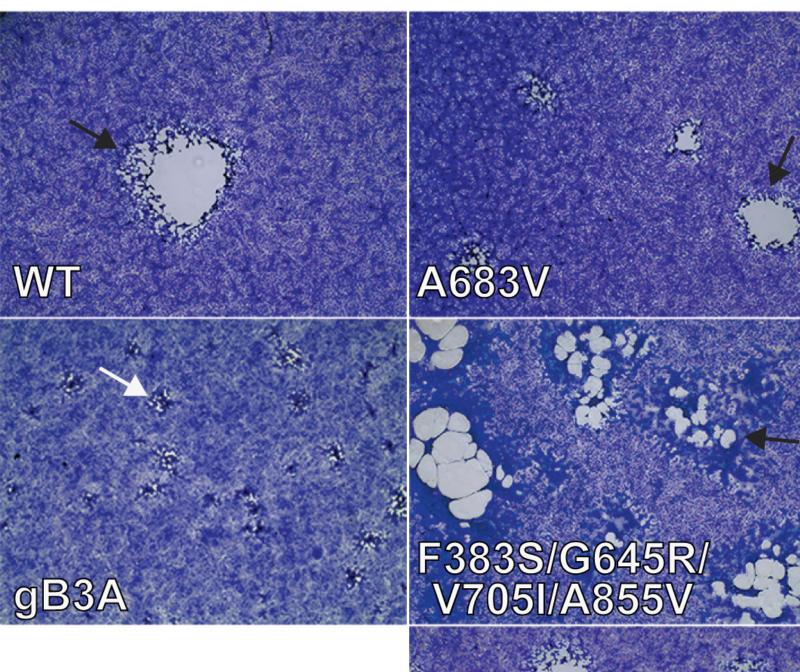
simplex virus fusogen gB. Nat Struct Mol Biol **25:**416-424.

557 25. Fan Z, Grantham ML, Smith MS, Anderson ES, Cardelli JA, Muggeridge MI.

- 558 2002. Truncation of herpes simplex virus type 2 glycoprotein B increases its cell
- 559 surface expression and activity in cell-cell fusion, but these properties are
- 560 unrelated. J Virol **76:**9271-9283.
- 56126.Ruel N, Zago A, Spear PG. 2006. Alanine substitution of conserved residues in
- 562 the cytoplasmic tail of herpes simplex virus gB can enhance or abolish cell fusion
- 563 activity and viral entry. Virology **346:**229-237.

564 27. Schroter C, Vallbracht M, Altenschmidt J, Kargoll S, Fuchs W, Klupp BG,

- 565 **Mettenleiter TC.** 2015. Mutations in Pseudorabies Virus Glycoproteins gB, gD,
- and gH Functionally Compensate for the Absence of gL. J Virol **90**:2264-2272.
- 567 28. Pertel P, Fridberg A, Parish ML, Spear PG. 2001. Cell fusion induced by
- 568 herpes simplex virus glycoproteins gB, gD, and gH-gL requires a gD receptor but
- 569 not necessarily heparan sulfate. Virology **279:**313-324.
- 570 29. Montgomery RI, Warner MS, Lum BJ, Spear PG. 1996. Herpes simplex virus-1
- 571 entry into cells mediated by a novel member of the TNF/NGF receptor family.
- 572 Cell **87:**427-436.
- 573 30. Fan Q, Longnecker R, Connolly SA. 2014. Substitution of herpes simplex virus
- 574 1 entry glycoproteins with those of saimiriine herpesvirus 1 reveals a gD-gH/gL
- 575 functional interaction and a region within the gD profusion domain that is critical
- 576 for fusion. Journal of virology **88:**6470-6482.
- 577 31. Lin E, Spear PG. 2007. Random linker-insertion mutagenesis to identify
- 578 functional domains of herpes simplex virus type 1 glycoprotein B. Proc Natl Acad
- 579 Sci USA **104:**13140-13145.



T509M/N709H

